

# The $p d \rightarrow \eta \text{}^3\text{He}$ reaction and bound $\eta$ state?. The $\rho B^* \bar{B}^*$ system

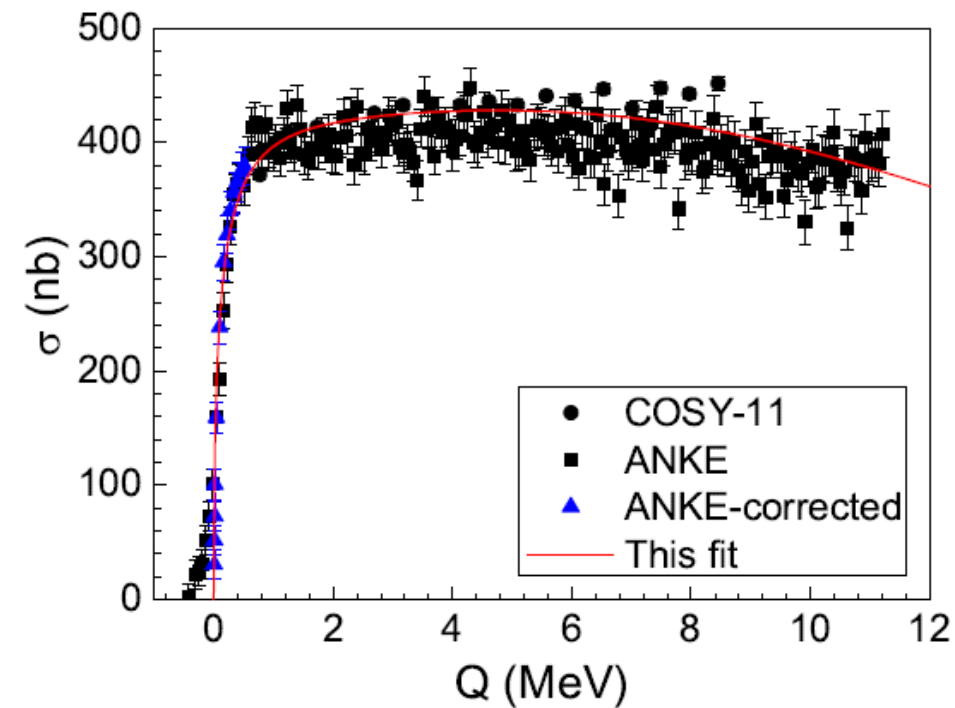
E. Oset, J.J. Xie, W. H. Liang, P. Moskal, M. Skurzok, C. Wilkin,  
M. Bayar, P. Fernandez Soler and Zhi Feng Sun

The  $p d \rightarrow \eta \text{}^3\text{He}$  reaction close to threshold

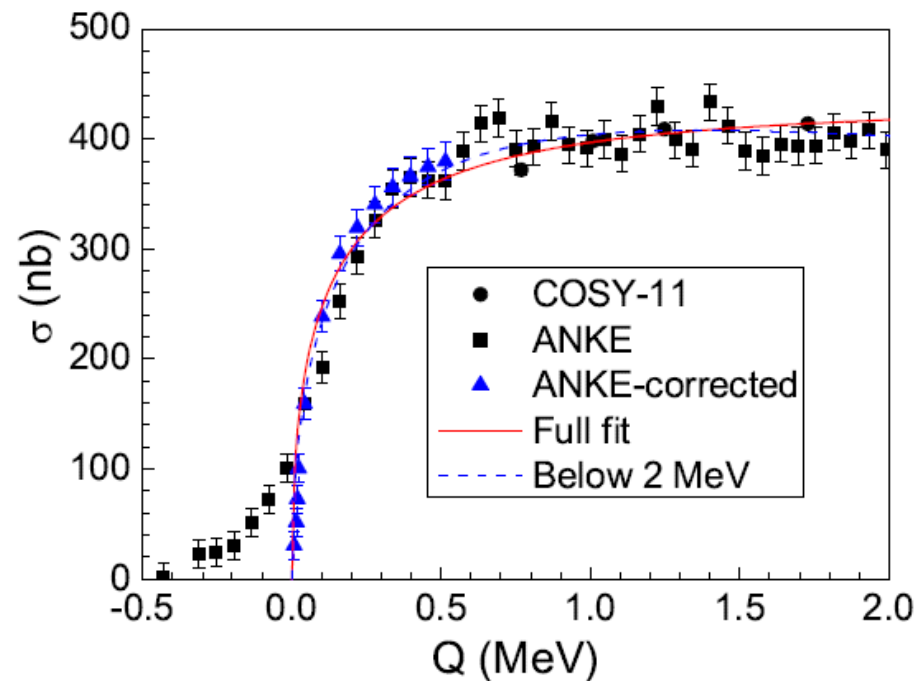
$\eta \text{}^3\text{He}$  bound state?

Study of the  $\rho B^* \bar{B}^*$  system. Bound state with  $J=3$ ,

# $pd \rightarrow \eta^3\text{He}$ total cross section



$$Q = \sqrt{s} - m_\eta - M_{^3\text{He}}$$



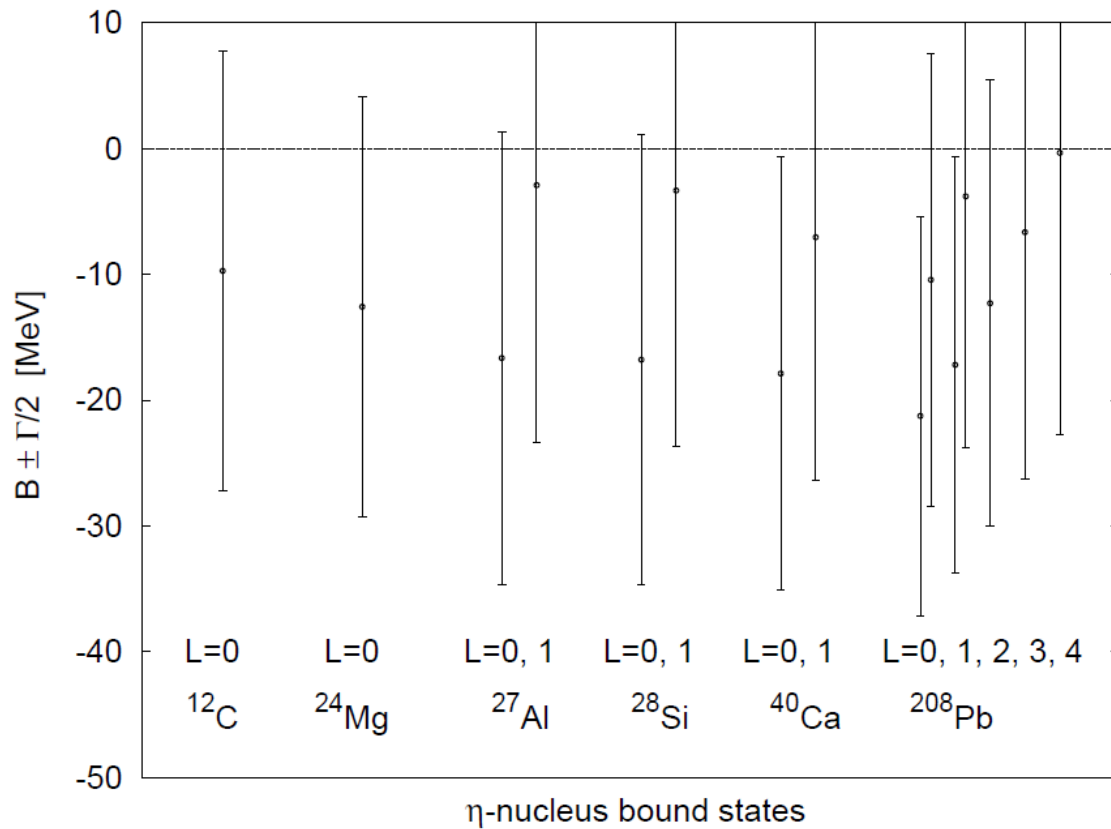
Fits to these data have been done before

T. Mersmann *et al.*, Phys. Rev. Lett. **98**, 242301 (2007)

C. Wilkin *et al.*, Phys. Lett. B **654**, 92 (2007)

All studies are done fitting a parametrized amplitude  
They get a small binding and very narrow width.

This is in contrast with all calculations, that give  $\Gamma > B$

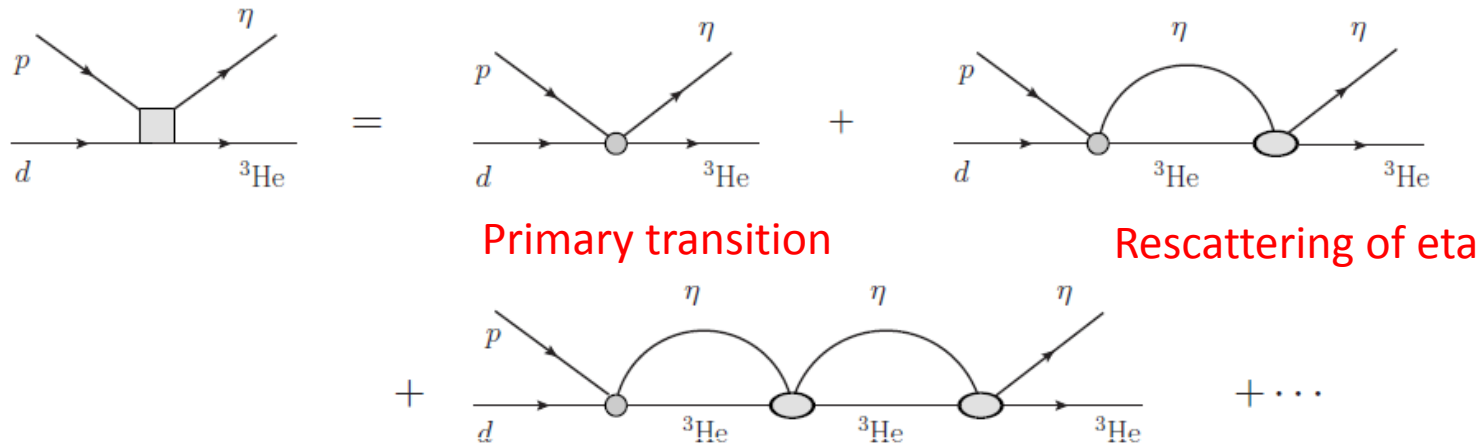


Garcia-Recio, Nieves, Inoue, E. O  
PLB (2002)

Other works suggest binding of  
1 MeV, or less, and  $\Gamma=15$  MeV,  
for  $^3\text{He}$

Barnea, Friedman and Gal,  
PLB (2015)

# Theoretical approach PRC (2017)



Primary transition

Rescattering of eta

Primary transition

$$V_P = A\vec{\epsilon} \cdot \vec{p} + iB(\vec{\epsilon} \times \vec{\sigma}) \cdot \vec{p},$$

S-wave in eta  $^3\text{He}$

$$V_{1P} = C\vec{\epsilon} \cdot \vec{p}_\eta + iD(\vec{\epsilon} \times \vec{\sigma}) \cdot \vec{p}_\eta.$$

P-wave in eta  $^3\text{He}$

$\eta$  rescattering

$$T = V + VGT,$$

$V$  is an optical potential, complex

Full transition amplitude

$$t = (V_P + V_{1P})(1+GT)$$

## Construction of T

In many body theory the low density theorem tells that for low densities,

$$V(\vec{r}) = t_{\eta N} \rho(\vec{r}) = 3t_{\eta N} \tilde{\rho}(\vec{r}),$$

with  $\tilde{\rho}(\vec{r})$  normalized to unity.

This is only used here to establish the range of the interaction

Momentum space

$$V(\vec{p}_\eta, \vec{p}'_\eta) = 3t_{\eta N} \int d^3\vec{r} \tilde{\rho}(\vec{r}) e^{i(\vec{p}_\eta - \vec{p}'_\eta) \cdot \vec{r}} = 3t_{\eta N} F(\vec{p}_\eta - \vec{p}'_\eta)$$
$$F(\vec{q}) = \int d^3\vec{r} \tilde{\rho}(\vec{r}) e^{i\vec{q} \cdot \vec{r}} \quad F(\vec{q}) = e^{-\beta^2 |\vec{q}|^2} \quad \beta^2 = 13.7 \text{ GeV}^{-2}.$$

s-wave projected

$$V(\vec{p}_\eta, \vec{p}'_\eta) = 3t_{\eta N} \frac{1}{2} \int_{-1}^1 d\cos\theta e^{-\beta^2 (|\vec{p}_\eta|^2 + |\vec{p}'_\eta|^2 - 2|\vec{p}_\eta||\vec{p}'_\eta|\cos\theta)}$$
$$= 3t_{\eta N} e^{-\beta^2 |\vec{p}_\eta|^2} e^{-\beta^2 |\vec{p}'_\eta|^2} \left[ 1 + \frac{1}{6} (2\beta^2 |\vec{p}_\eta||\vec{p}'_\eta|)^2 + \dots \right].$$

The term [...] is essentially 1 in the range of study and, thus, **the potential is separable**

$$T(\vec{p}_\eta, \vec{p}'_\eta) = \tilde{V} e^{-\beta^2 |\vec{p}_\eta|^2} e^{-\beta^2 |\vec{p}'_\eta|^2} + \int \frac{d^3 \vec{q}}{(2\pi)^3} \frac{M_{3\text{He}}}{2\omega_\eta(\vec{q}) E_{3\text{He}}(\vec{q})} \frac{\tilde{V} e^{-\beta^2 |\vec{p}_\eta|^2} e^{-\beta^2 |\vec{q}|^2}}{\sqrt{s} - \omega_\eta(\vec{q}) - E_{3\text{He}}(\vec{q}) + i\epsilon} \tilde{T} e^{-\beta^2 |\vec{q}|^2} e^{-\beta^2 |\vec{p}'_\eta|^2}$$

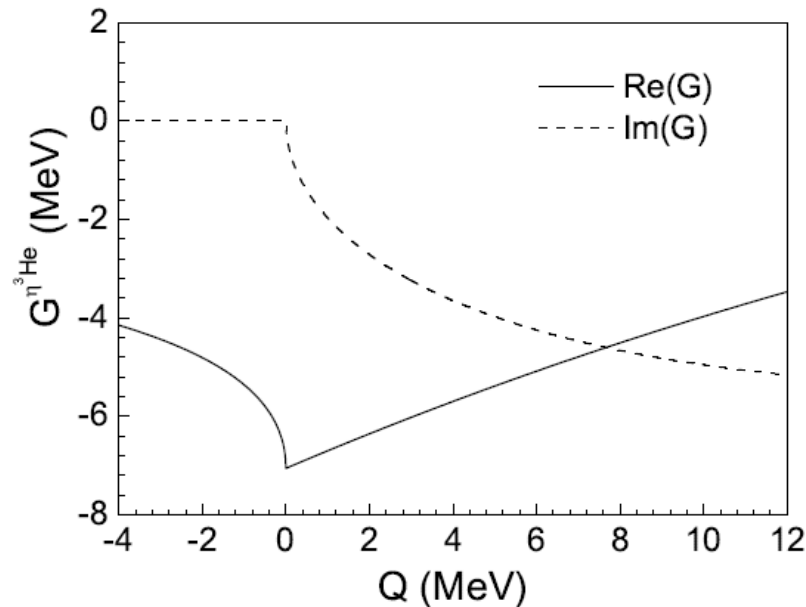
But we do not take

Take instead

$$3t_{\eta N} e^{-\beta^2 |\vec{p}_\eta|^2} e^{-\beta^2 |\vec{p}'_\eta|^2} \longrightarrow \tilde{V} e^{-\beta^2 |\vec{p}_\eta|^2} e^{-\beta^2 |\vec{p}'_\eta|^2} \quad T(\vec{p}_\eta, \vec{p}'_\eta) = \tilde{T} e^{-\beta^2 |\vec{p}_\eta|^2} e^{-\beta^2 |\vec{p}'_\eta|^2}$$

$$\tilde{T} = \tilde{V} + \tilde{V} G \tilde{T} \quad \tilde{V} \quad \text{will be a fit parameter}$$

$$G = \int \frac{d^3 \vec{q}}{(2\pi)^3} \frac{1}{2\omega_\eta(\vec{q})} \frac{M_{3\text{He}}}{E_{3\text{He}}(\vec{q})} \frac{e^{-2\beta^2 |\vec{q}|^2}}{\sqrt{s} - \omega_\eta(\vec{q}) - E_{3\text{He}}(\vec{q}) + i\epsilon}$$



$$a_{\eta N} = \frac{1}{4\pi} \frac{m_N}{\sqrt{s_{\eta N}}} t_{\eta N} \Big|_{\sqrt{s_{\eta N}}=m_N+m_\eta}$$

$$a_{\eta^3\text{He}} = \frac{1}{4\pi} \frac{M_{^3\text{He}}}{\sqrt{s}} T \Big|_{\sqrt{s}=M_{^3\text{He}}+m_\eta}$$

$$a'_{\eta N} = \frac{1}{4\pi} \frac{m_N}{\sqrt{s_{\eta N}}} \frac{\tilde{V}}{3} \Big|_{\sqrt{s_{\eta N}}=m_N+m_\eta}$$

S-wave  $t_{dp \rightarrow \eta^3\text{He}} = V_P e^{-\beta^2 |\vec{p}_\eta|^2} + V_P G \tilde{T} e^{-\beta^2 |\vec{p}_\eta|^2} = V_P e^{-\beta^2 |\vec{p}_\eta|^2} (1 + G \tilde{T}) = \frac{V_P e^{-\beta^2 |\vec{p}_\eta|^2}}{1 - \tilde{V} G},$

$$\sigma = \frac{m_p M_{^3\text{He}}}{12\pi s} (|A'|^2 + 2|B'|^2) |\vec{p}_\eta| |\vec{p}| e^{-2\beta^2 |\vec{p}_\eta|^2}$$

$$A' = \frac{A}{1 - \tilde{V} G}; \quad B' = \frac{B}{1 - \tilde{V} G}.$$

## INCLUSION OF $p$ -WAVE

$$V_{1P} = C\vec{\epsilon} \cdot \vec{p}_\eta + iD(\vec{\epsilon} \times \vec{\sigma}) \cdot \vec{p}_\eta$$

$$\frac{d\sigma}{d\Omega} = \frac{m_p M_{3\text{He}}}{48\pi^2 s} \frac{|\vec{p}_\eta|}{|\vec{p}|} \left( (|A'|^2 + 2|B'|^2)|\vec{p}|^2 e^{-\beta^2|\vec{p}_\eta|^2} + (|C|^2 + 2|D|^2)|\vec{p}_\eta|^2 + 2\text{Re}(A'C^* + 2B'D^*)|\vec{p}||\vec{p}_\eta|\cos(\theta_\eta) \right),$$

Asymmetry

$$\alpha = \frac{d}{d(\cos\theta_\eta)} \ln\left(\frac{d\sigma}{d\Omega}\right) \Big|_{\cos(\theta_\eta)=0}.$$

$$\alpha = \frac{2\text{Re}(A'C^* + 2B'D^*)|\vec{p}||\vec{p}_\eta|}{(|A'|^2 + 2|B'|^2)|\vec{p}|^2 e^{-2\beta^2|\vec{p}_\eta|^2} + (|C|^2 + 2|D|^2)|\vec{p}_\eta|^2}.$$

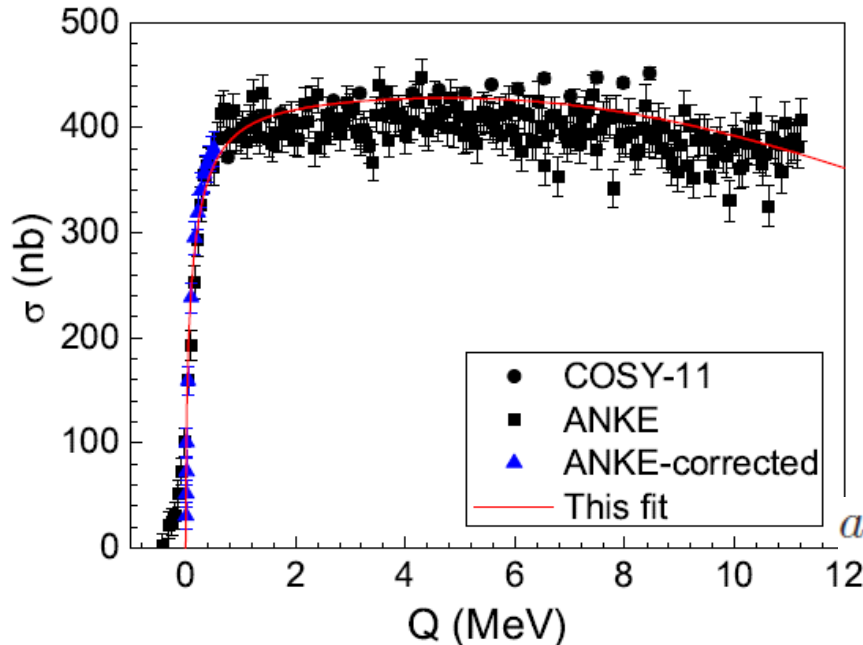
$$\sigma = \frac{m_p M_{3\text{He}}}{12\pi s} \frac{|\vec{p}_\eta|}{|\vec{p}|} \left( (|A'|^2 + 2|B'|^2)|\vec{p}|^2 e^{-2\beta^2|\vec{p}_\eta|^2} + (|C|^2 + 2|D|^2)|\vec{p}_\eta|^2 \right)$$

## RESULTS

Next, we perform six-parameter ( $A = B = r_A$ ,  $C = D = r_C e^{i\theta}(1 + \beta Q)$ , and  $\tilde{V} = \text{Re}(V) + i\text{Im}(V)$ )  $\chi^2$  fits to the experimental data on the total cross sections and asymmetry

Parameters	Fitted values	parameters	Fitted values
$r_A [\text{MeV}^{-2}]$	$(9.44 \pm 2.85) \times 10^{-7}$	$\beta [\text{MeV}^{-1}]$	$(-5.25 \pm 2.47) \times 10^{-2}$
$r_C [\text{MeV}^{-2}]$	$(6.85 \pm 4.79) \times 10^{-6}$	$\text{Re}(V) [\text{MeV}^{-1}]$	$(-14.58 \pm 6.04) \times 10^{-2}$
$\theta [\text{degree}]$	$347 \pm 29$	$\text{Im}(V) [\text{MeV}^{-1}]$	$(-5.37 \pm 2.31) \times 10^{-2}$

Exp. support for  $A=B$ ,  $C=D$  from Berger et al. PRL 1988,  $|A/B|=1$  from Papenbrock, PLB 2014



$$a'_{\eta N} = -(0.48 \pm 0.20) - i(0.18 \pm 0.08) \text{ fm.}$$

$$a_{\eta N} = (-0.264 - i0.245) \text{ fm in Ref. [14].}$$

$$a_{\eta N} = (-0.20 - i0.26) \text{ fm in Ref. [5].}$$

$$a_{\eta N} = (-0.87 - i0.27) \text{ fm} \quad [22]$$

$$a_{\eta N} = (-0.691 - i0.174) \text{ fm} \quad [23]$$

$$a_{\eta N} = (-0.968 - i0.281) \text{ fm}$$

$$a_{\eta N} = (-0.910 \pm 0.050 + i(0.290 \pm 0.04)) \text{ fm} [24]$$

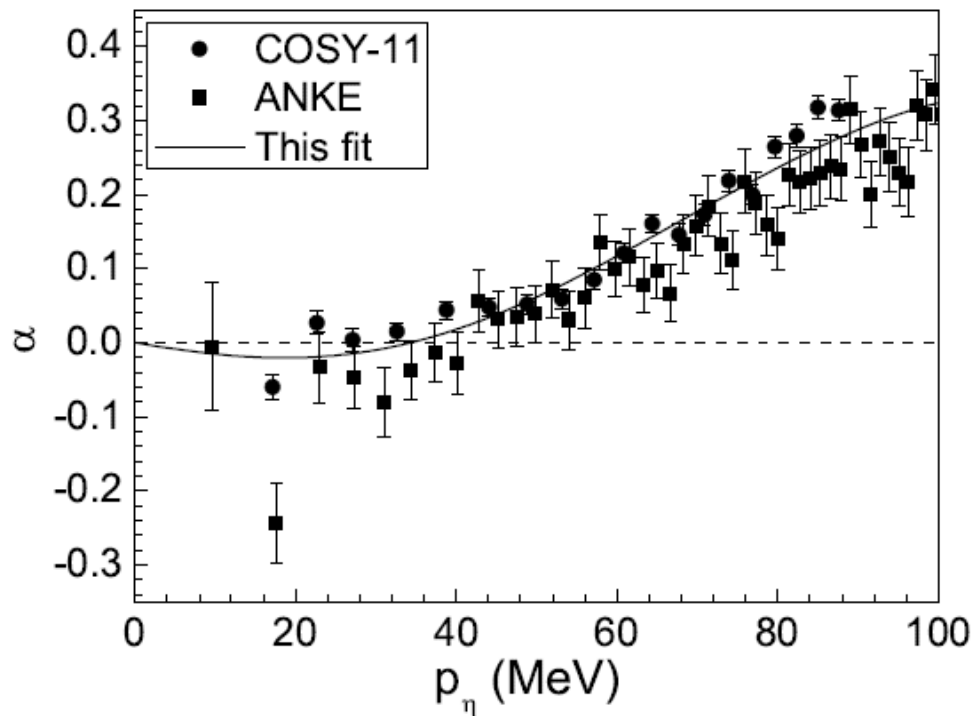
[5] T. Waas, N. Kaiser and W. Weise, *Phys. Lett. B* **379**, 34 (1996).

[14] T. Inoue and E. Oset, *Nucl. Phys. A* **710**, 354 (2002)

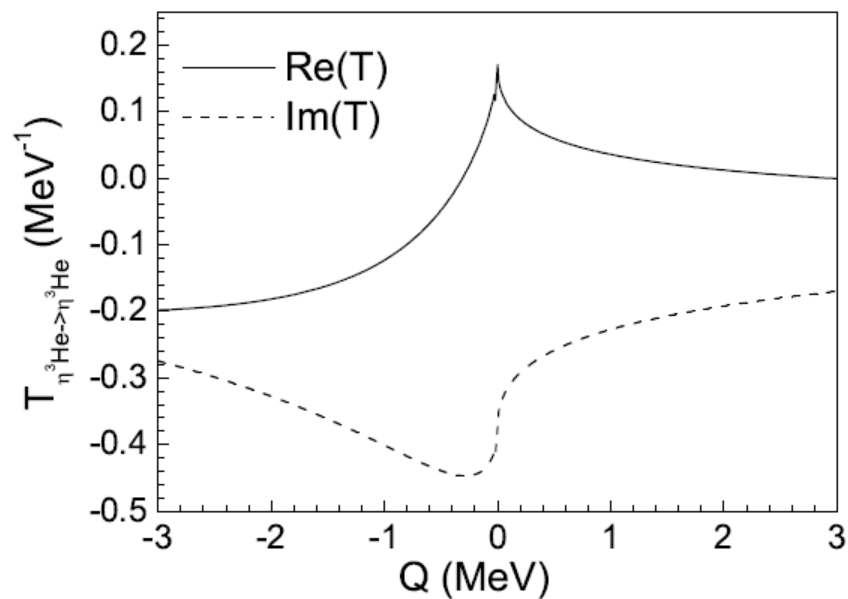
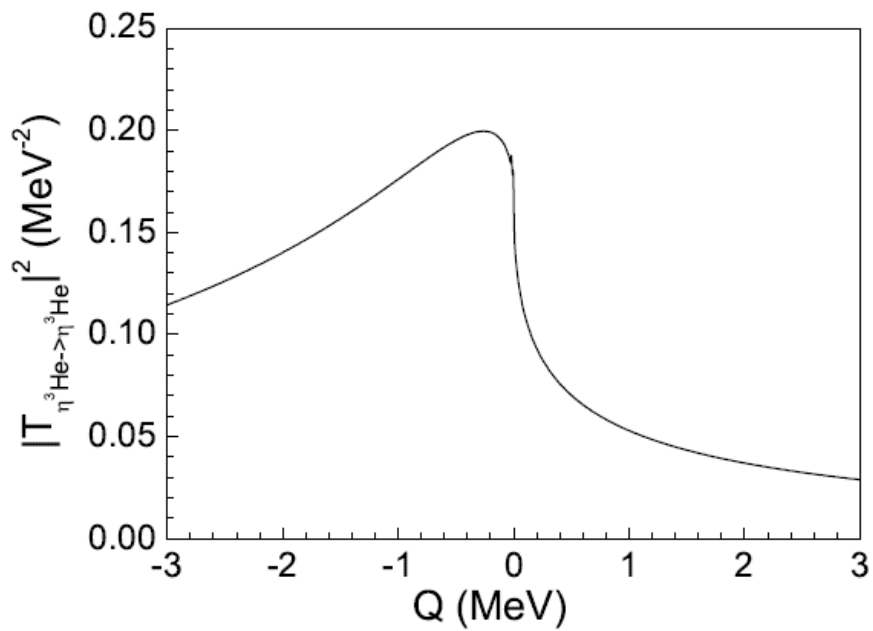
[22] A. M. Green and S. Wycech, *Phys. Rev. C* **60**, 035208 (1999)

[23] M. Batinic, I. Slaus and A. Svarc, *Phys. Rev. C* **52**, 2188 (1995).

[24] M. Batinic, I. Slaus, A. Svarc and B. M. K. Nefkens, *Phys. Rev. C* **51**, 2310 (1995) Erratum:  
[*Phys. Rev. C* **57**, 1004 (1998)].



## Results



$$T = \frac{g^2}{\sqrt{s} - M_R + i\Gamma/2} = \frac{g^2(\sqrt{s} - M_R)}{(\sqrt{s} - M_R)^2 + \Gamma^2/4} - i \frac{g^2\Gamma/2}{(\sqrt{s} - M_R)^2 + \Gamma^2/4}$$

$$B = 0.3 \text{ MeV with } \Gamma = 3 \text{ MeV.}$$

But if one searches for poles, the pole is at  $Q = (1.5 - i 0.7) \text{ MeV}$ , in the positive energy side.

This is quite common in Particle Physics: for instance the Roper has  
 BW mass 1430 MeV, BW width 350 MeV  
 Pole position  $(1365 - i 190/2) \text{ MeV}$

But what one sees experimentally is the BW form in the real axis. This is the novel message of the present study, showing that there is an approximate BW amplitude below threshold for  $\eta^3\text{He}$ , which in principle is amenable of experimental observation.

An immediate repercussion is that the  $\eta^3\text{He}$  scattering length has a positive real part

$$a_{\eta^3\text{He}} = [(2.23 \pm 1.29) - i(4.89 \pm 0.57)] \text{ fm.}$$

If the BW mass were above threshold, the real part would be negative!!

The amplitudes are observable, so is  $a_{\eta^3\text{He}}$ . Yet, different analyses give different results

$$a_{\eta^3\text{He}} = (\pm 10.9 - i 1.0) \text{ fm} \quad \text{ANKE, Wilkin et al, PLB 2007}$$

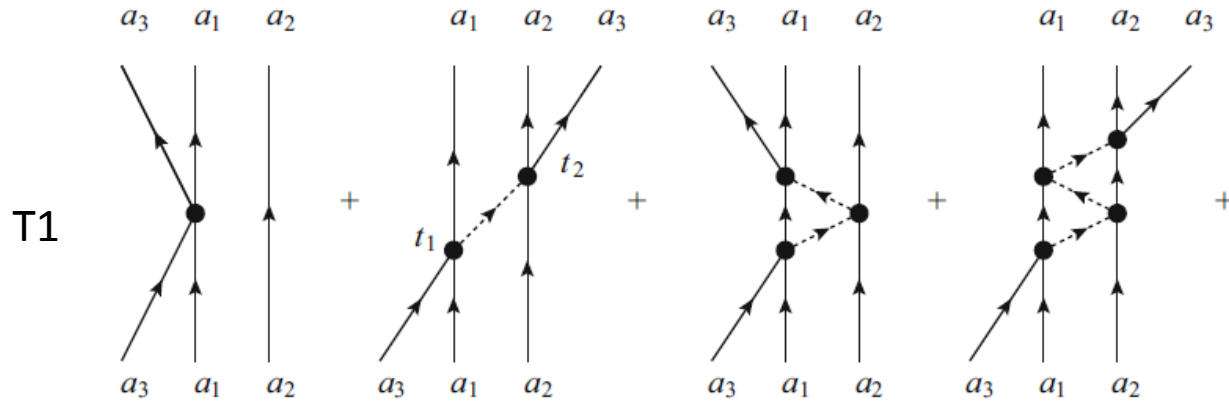
$$a_{\eta^3\text{He}} = (\pm 2.9 - i 3.2) \text{ fm}, \quad \text{COSY-11, from same raw data without taking beam smearing effects into account Smysky PLB 2007}$$

$$a_{\eta^3\text{He}} = [(-4.3 \pm 0.3) - i(0.5 \pm 0.5)] \text{ fm} \quad \text{Sibirtsev et al. EPJA 2002}$$

**Our results:**  $a_{\eta^3\text{He}} = [(2.23 \pm 1.29) - i(4.89 \pm 0.57)] \text{ fm}.$

# States of $\rho B^* \bar{B}^*$ with $J = 3$ within the fixed center approximation to Faddeev equations

M. Bayar, P. Fernandez-Soler, Zhi Feng Sun, E. O. EPJA 2016



$$T_1 = t_1 + t_1 G_0 T_2,$$

$$T_2 = t_2 + t_2 G_0 T_1.$$

$$T = T_1 + T_2$$

$$|\rho B^* \bar{B}^*, I = 1, I_3 = 1\rangle = |I = 1, I_3 = 1\rangle_\rho$$

$$\otimes |I = 0, I_3 = 0\rangle_{B^* \bar{B}^*}$$

$$= |I = 1, I_3 = 1\rangle_\rho$$

$$t_j(I = 1) = \frac{2}{3} \hat{t}_j^{I=3/2} + \frac{1}{3} \hat{t}_j^{I=1/2}, \quad j = 1, 2.$$

(1)  $\rho B^*$ , (2)  $\rho B^* \bar{B}^*$

$$\otimes \left\{ \frac{1}{\sqrt{2}} \left( \left| I_3 = \frac{1}{2} \right\rangle_{B^*} \left| I_3 = -\frac{1}{2} \right\rangle_{\bar{B}^*} - \left| I_3 = -\frac{1}{2} \right\rangle_{B^*} \left| I_3 = \frac{1}{2} \right\rangle_{\bar{B}^*} \right) \right\}.$$

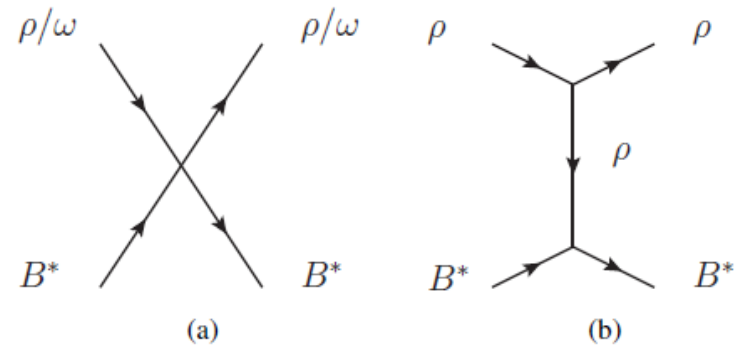
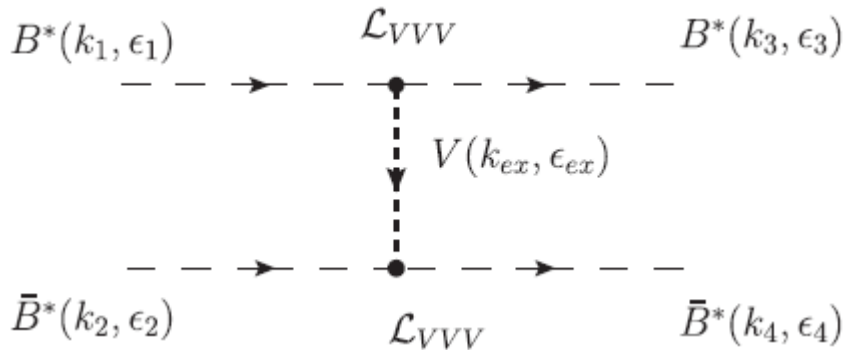
$$G_0(q^0) = \frac{1}{2M_c} \int_{\mathbb{R}^3} \frac{d^3q}{(2\pi)^3} F_R(\vec{q}^2) \frac{1}{(q^0)^2 - \vec{q}^2 - m_{a_3}^2 + i\epsilon}$$

$$\tilde{t}_i = t_i \left( \frac{\omega(c)\omega'(c)}{\omega(a_i)\omega'(a_i)} \right)^{1/2} \approx t_i \frac{M_c}{m_{a_i}}$$

$$T = T_1 + T_2 = \frac{\tilde{t}_1 + \tilde{t}_2 + 2\tilde{t}_1\tilde{t}_2G_0}{1 - \tilde{t}_1\tilde{t}_2G_0^2} \quad \tilde{t}_1 = \tilde{t}_2 \quad T = \frac{2\tilde{t}_1}{1 - \tilde{t}_1G_0}$$

Input needed: Wave function for  $B^*$   $\bar{B}^*$  to evaluate the  $FR(q^2)$  form factor  
 Interaction of  $\rho$   $B$  and  $\rho$   $\bar{B}^*$  (same)

In all cases the local hidden gauge approach is used (Bando et al. ), with the exchange of vector mesons

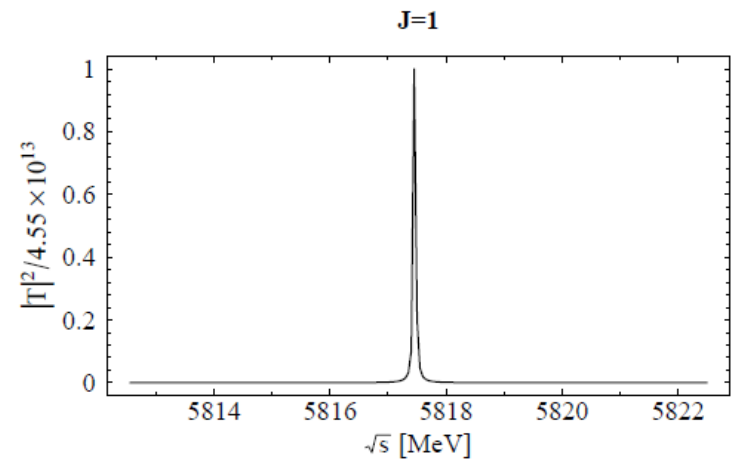
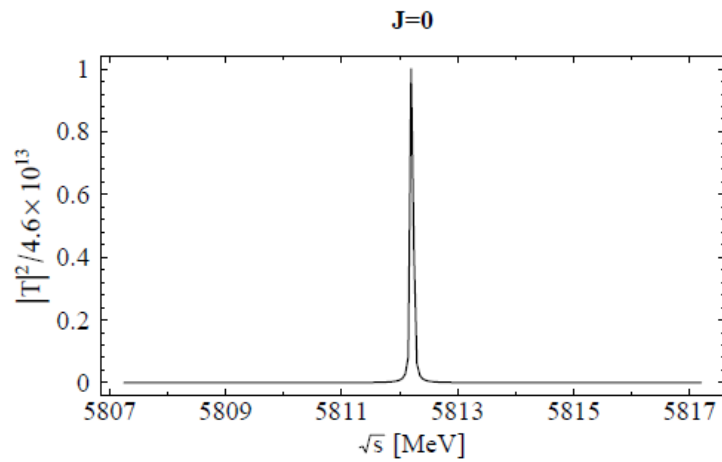


$$T = [1 - VG]^{-1}V$$

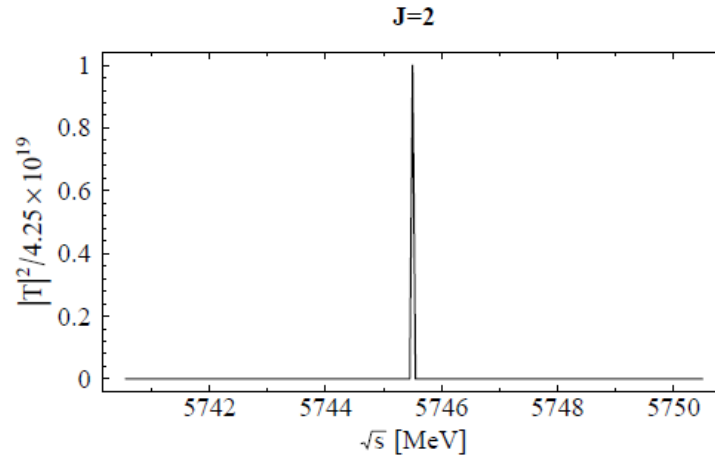
TABLE I. The couplings to various channels for the poles in the  $J^{PC} = 2^{++}$  channel for  $q_{\max} = 415$  MeV (left panel) and  $q_{\max} = 830$  MeV (right panel); all units are in MeV.

10613	$B^*\bar{B}^*$	$B_s^*\bar{B}_s^*$	10469	$B^*\bar{B}^*$	$B_s^*\bar{B}_s^*$
$g_i$	86168	45864	$g_i$	174393	92843

A. Ozpineci,  
C. Wen Xiao, E.O.  
PRD 2013



$\rho B^*$



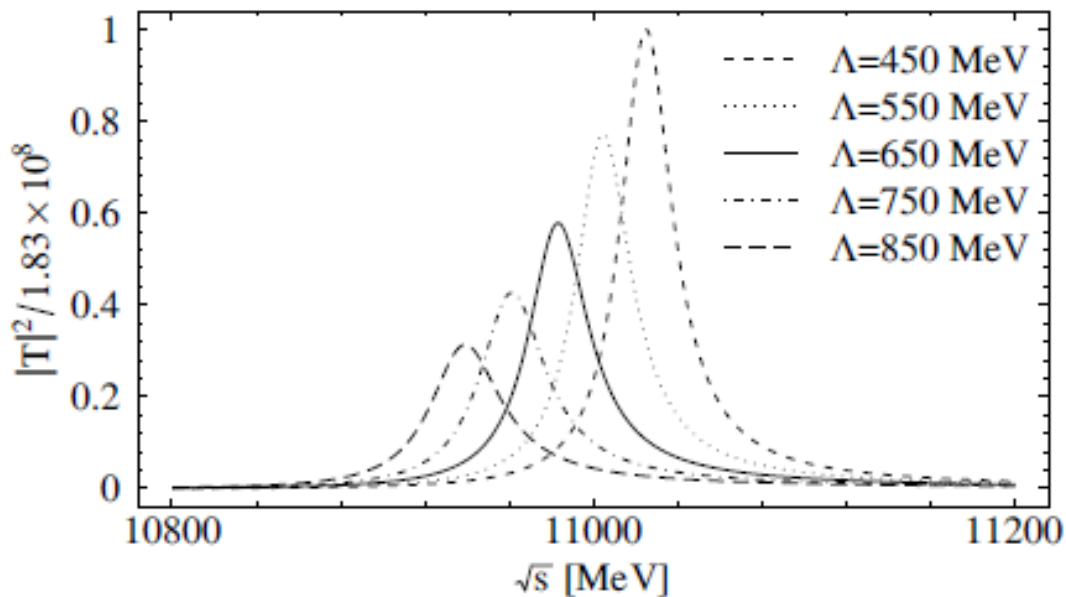
P. Fernandez, Z. F. Sun  
J.Nieves, E. O, EPJC 2016

TABLE III: Summary of the states found in the  $\rho(\omega)B^*$  and  $\rho B$  interaction.

Main channel	$I(J^P)$	$M$ [MeV]	$\Gamma$ [MeV]	Main decay channel	Exp ( $M, \Gamma$ ) [MeV]
$\rho B^*$	$\frac{1}{2}(0^+)$	5812	25 – 45	$\pi B$	
$\rho B^*$	$\frac{1}{2}(1^+)$	5817	0		
$\rho B^*$	$\frac{1}{2}(2^+)$	5745	25 – 35	$\pi B$	$(5743 \pm 5, 23_{-11}^{+5})$
$\rho B$	$\frac{1}{2}(1^+)$	5728	18 – 24	$\pi B^*$	$(5723.5 \pm 2, -)$

**Table 1.** The mass and width of the  $I(J^{PC}) = 1(3^{--})$  state found in the  $\rho B^* \bar{B}^*$  interaction in the FCA to Faddeev equations.

$\Lambda$ [MeV]	Mass [MeV]	Width [MeV]
450	11025	30
550	11004	32
650	10983	35
750	10962	38
850	10939	41



## Conclusions

--- The new analysis of the  $p d \rightarrow \eta \ ^3\text{He}$  close to threshold has brought new information concerning the possible  $\eta \ ^3\text{He}$  state: The  $\eta \ ^3\text{He} \rightarrow \eta \ ^3\text{He}$  amplitude develops a local BW structure below threshold with energy  $Q = -0.3 \text{ MeV}$ ,  $\Gamma = 3 \text{ MeV}$ . Yet, the pole is in the positive energy side

One consequence of this structure is a positive  $\eta \ ^3\text{He}$  scattering length  
 $a_{\eta^3\text{He}} = 2.2 - i 4.9 \text{ fm}$ .

## PRECISE DATA AND A NEW ANALYSIS METHOD, LEAD TO ALL THIS INFORMATION

-----Concerning the  $\rho B^* \bar{B}^*$  state with  $J=3$ , predictions are made that such state should exist with a mass around 11000 MeV and a width around 30 MeV

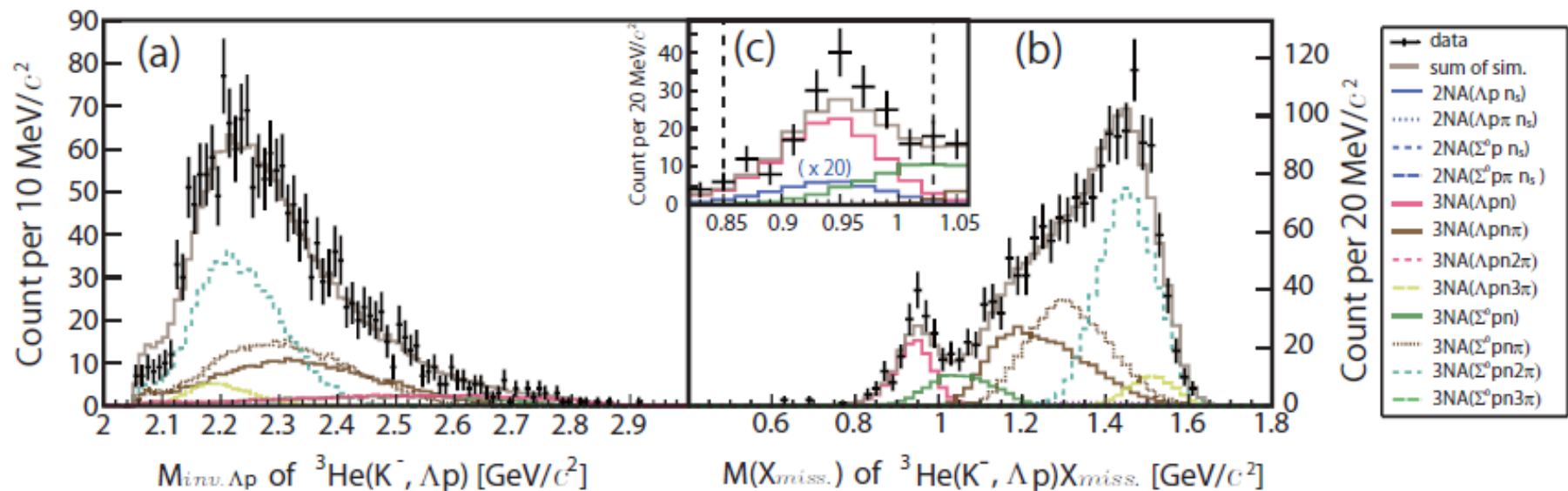
We should note that  $\rho_3(1690) (3^{--})$ ,  $f_4(2050) (4^{++})$ ,  $\rho_5(2350) (5^{--})$  and  $f_6(2510) (6^{++})$  exist and are described as multirho states in Roca, Oset, PRD 2010

Similarly  $K_2^*(1430)$ ,  $K_3^*(1780)$ ,  $K_4^*(2045)$ ,  $K_5^*(2380)$  also exist and are described as  $K^*$  multirho states in Yamagata, Roca, Oset PRD 2010

States with  $J=3$  from the interaction of vector mesons in the heavy sector should also exist, and we encourage their search.

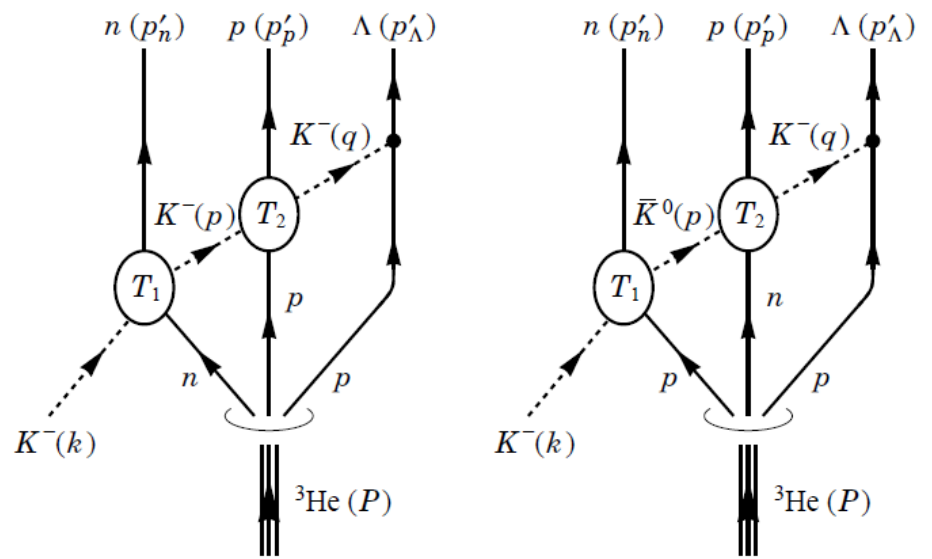
# On the structure observed in the in-flight ${}^3\text{He}(K^-, \Lambda p)n$ reaction at J-PARC

Takayasu Sekihara<sup>1,\*</sup> Eulogio Oset<sup>2</sup>, and Angels Ramos<sup>3</sup>



**Structure near  $\kappa \rightarrow p + p$  threshold in the in-flight  ${}^3\text{He}(K^-, \Lambda p)n$  reaction**

# Theoretical interpretation



If we want to produce a Kbar NN system, we must get the first rescattered Kbar as much at rest as possible . This happens at 1Gev/c and backward scattering in CM. The n goes forward in the lab system.

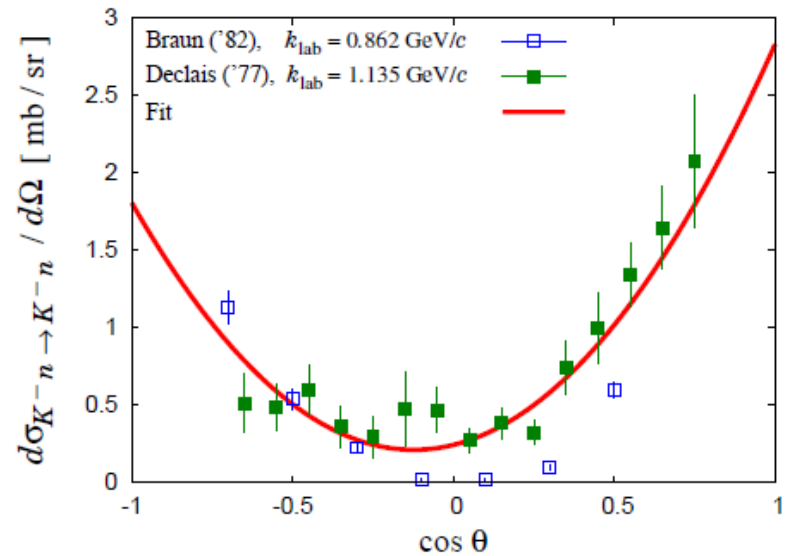
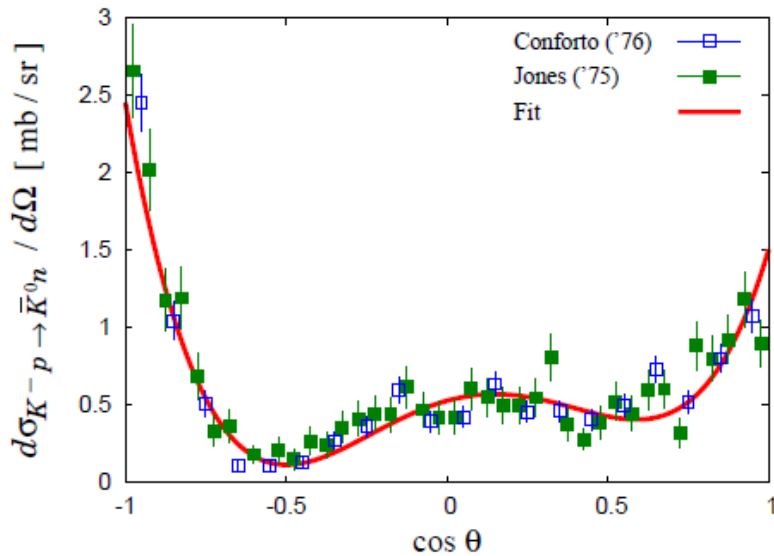


Fig. B1 Differential cross sections of the  $K^-p \rightarrow \bar{K}^0n$  (left) and  $K^-n \rightarrow \bar{K}^-n$  (right)

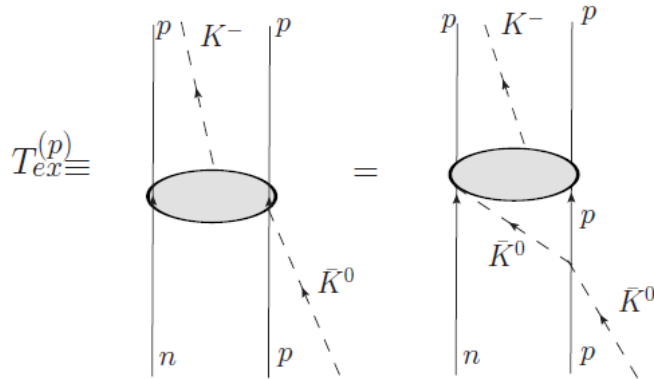
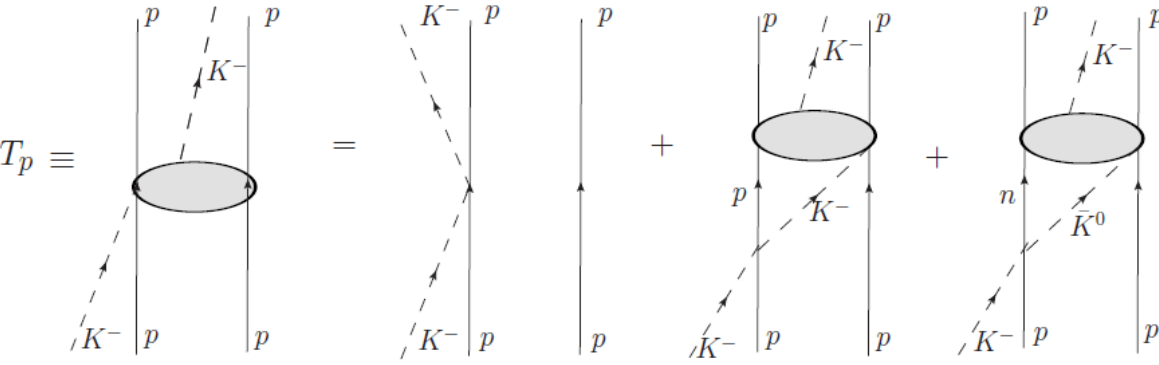
$$\begin{aligned}
|{}^3\text{He}(\chi)\rangle = \frac{1}{\sqrt{6}}\tilde{\Psi}(p_\lambda, p_\rho) [ & |n(p_1, \chi)p(p_2, \chi_\uparrow)p(p_3, \chi_\downarrow)\rangle - |n(p_1, \chi)p(p_3, \chi_\downarrow)p(p_2, \chi_\uparrow)\rangle \\
& - |p(p_2, \chi_\uparrow)n(p_1, \chi)p(p_3, \chi_\downarrow)\rangle + |p(p_3, \chi_\downarrow)n(p_1, \chi)p(p_2, \chi_\uparrow)\rangle \\
& + |p(p_2, \chi_\uparrow)p(p_3, \chi_\downarrow)n(p_1, \chi)\rangle - |p(p_3, \chi_\downarrow)p(p_2, \chi_\uparrow)n(p_1, \chi)\rangle ]
\end{aligned}$$

Different orders of the interactions amount to a factor 6 in the cross section when this wave function is explicitly considered. Jacobi coordinates are used for the 3He.

$$\begin{aligned}
-i\mathcal{T}_1 = & \int \frac{d^3q}{(2\pi)^3} \frac{i}{(q^0)^2 - \omega_{K^-}(\mathbf{q})^2} \int \frac{d^3p}{(2\pi)^3} \frac{i}{(p^0)^2 - \omega_{K^-}(\mathbf{p})^2 + im_{K^-}\Gamma_K} \tilde{\Psi}(p_\lambda, p_\rho) \\
& \times \left[ -i\chi_p^\dagger T_2^{(K^-p \rightarrow K^-p)}(w_2)\chi_\uparrow \right] \left[ -i\chi_n^\dagger T_1^{(K^-n \rightarrow K^-n)}(w_1, \cos\theta_1)\chi \right] \\
& \times \left[ \tilde{V}\mathcal{F}(\mathbf{q})\mathbf{q} \left( \chi_\Lambda^\dagger \boldsymbol{\sigma} \chi_\downarrow \right) \right],
\end{aligned}$$

We introduce a width for the Kbar to account for Kbar absorption by two nucleons based on the work of Bayar, Oset PRC 88 , 044003 (2013)

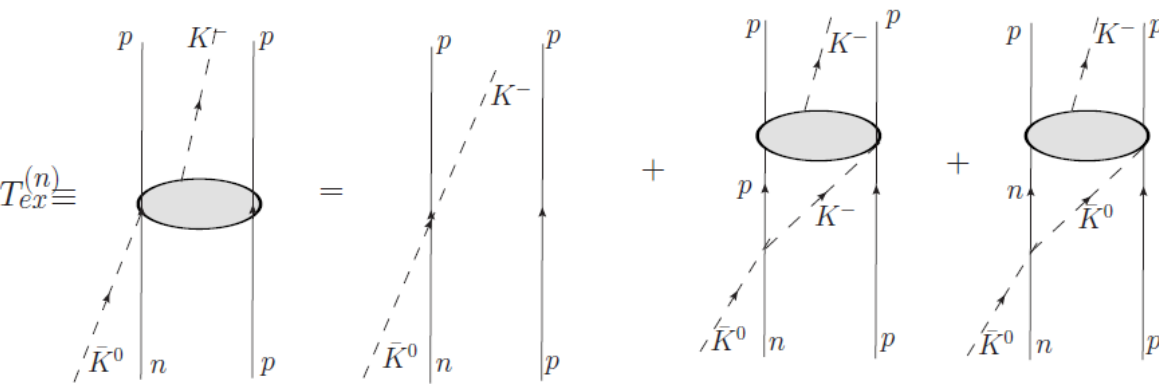
# $\bar{K}NN$ Absorption within the Framework of the Fixed Center Approximation to Faddeev equations



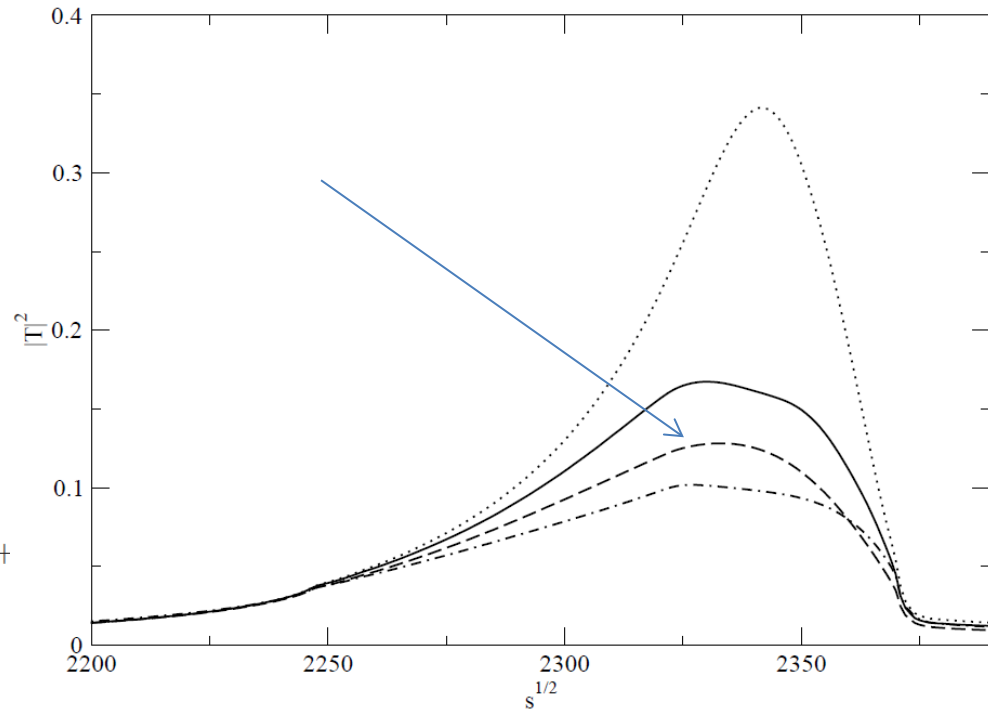
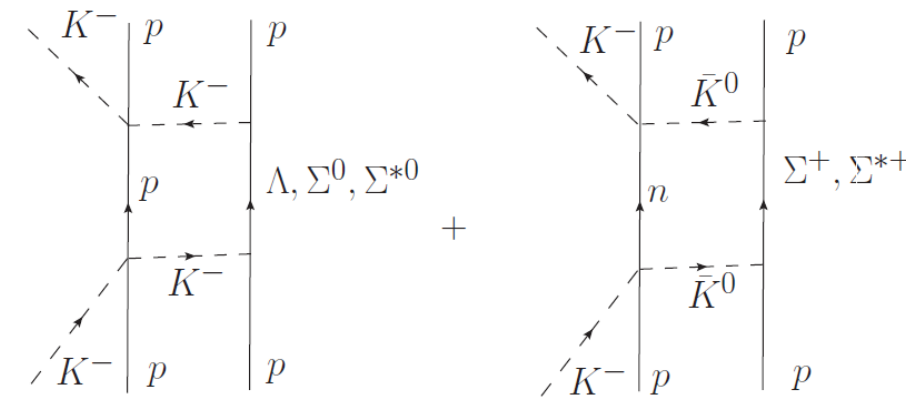
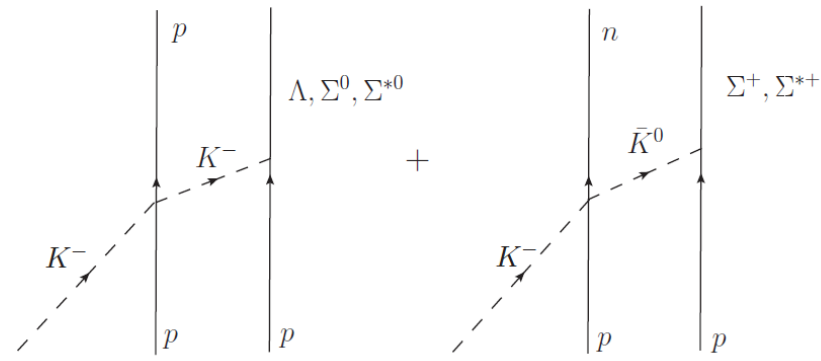
$$T_p = t_p + t_p G_0 T_p + t_{ex} G_0 T_{ex}^{(p)}$$

$$T_{ex}^{(p)} = t_0^{(p)} G_0 T_{ex}^{(n)}$$

$$T_{ex}^{(n)} = t_{ex} + t_{ex} G_0 T_p + t_0^{(n)} G_0 T_{ex}^{(p)}$$

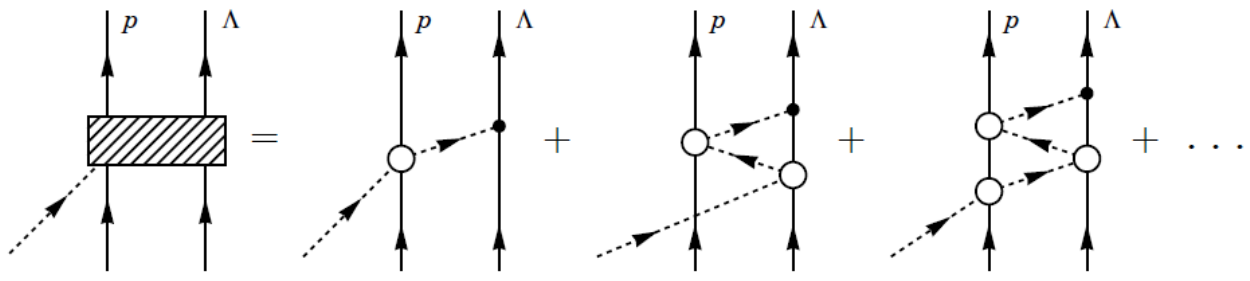
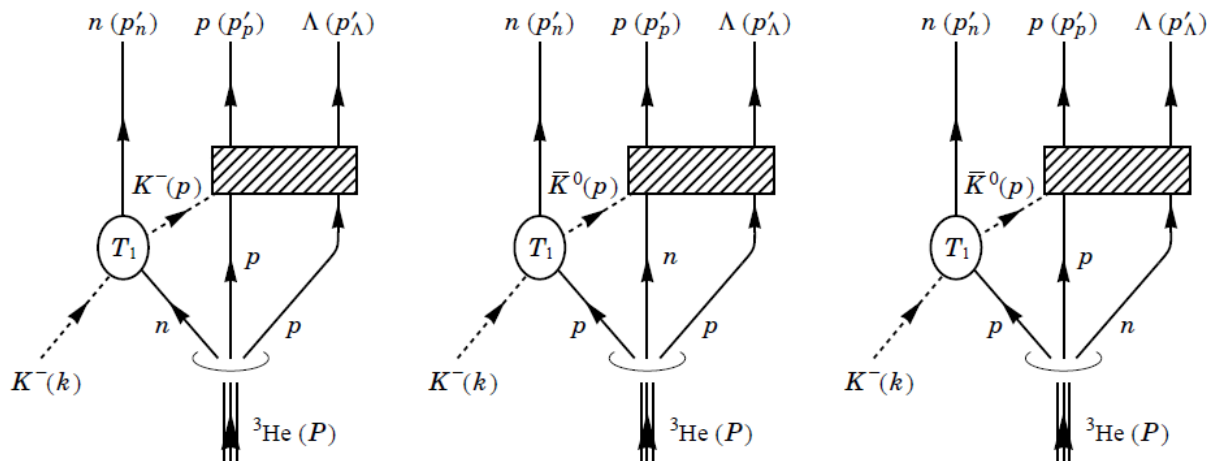


$$G_0 = \int \frac{d^3 q}{(2\pi)^3} F_{NN}(q) \frac{1}{q^0{}^2 - \vec{q}^2 - m_K^2 + i\epsilon}$$



$B = 20 \text{ MeV}, \Gamma = 75\text{-}80 \text{ MeV}$

In Bayar's paper it is shown that this can be taken into account taking a  $K$ bar width of about 15 MeV. This is the only work in which the  $K$ bar absorption by two nucleons is evaluated. It provides about 30 MeV more to the width of the  $K$ bar NN state.



Six configurations:  $K^-pp$ ,  $\bar{K}^0np$ ,  $\bar{K}^0pn$ ,  $ppK^-$ ,  $np\bar{K}^0$ , and  $pn\bar{K}^0$

$$T_{ij}^{\text{FCA}} = V_{ij}^{\text{FCA}} + \sum_{k=1}^6 \tilde{V}_{ik}^{\text{FCA}} G_0 T_{kj}^{\text{FCA}} = \sum_{k=1}^6 \left[ 1 - \tilde{V}^{\text{FCA}} G_0 \right]^{-1}_{ik} V_{kj}^{\text{FCA}}$$

with

$$V^{\text{FCA}} = \begin{pmatrix} t_1 & t_2 & 0 & 0 & 0 & 0 \\ t_2 & t_3 & 0 & 0 & 0 & 0 \\ 0 & 0 & t_4 & 0 & 0 & 0 \\ 0 & 0 & 0 & t_1 & 0 & t_2 \\ 0 & 0 & 0 & 0 & t_4 & 0 \\ 0 & 0 & 0 & t_2 & 0 & t_3 \end{pmatrix}, \quad \tilde{V}^{\text{FCA}} = \begin{pmatrix} 0 & 0 & 0 & t_1 & t_2 & 0 \\ 0 & 0 & 0 & t_2 & t_3 & 0 \\ 0 & 0 & 0 & 0 & 0 & t_4 \\ t_1 & 0 & t_2 & 0 & 0 & 0 \\ 0 & t_4 & 0 & 0 & 0 & 0 \\ t_2 & 0 & t_3 & 0 & 0 & 0 \end{pmatrix}.$$

$$t_1(M_{\Lambda p}) = T_{K^-p \rightarrow K^-p}^{\text{ChUA}}$$

$$t_2(M_{\Lambda p}) = T_{K^-p \rightarrow \bar{K}^0n}^{\text{ChUA}}$$

$$t_3(M_{\Lambda p}) = T_{\bar{K}^0n \rightarrow \bar{K}^0n}^{\text{ChUA}}$$

$$t_4(M_{\Lambda p}) = T_{\bar{K}^0p \rightarrow \bar{K}^0p}^{\text{ChUA}}$$

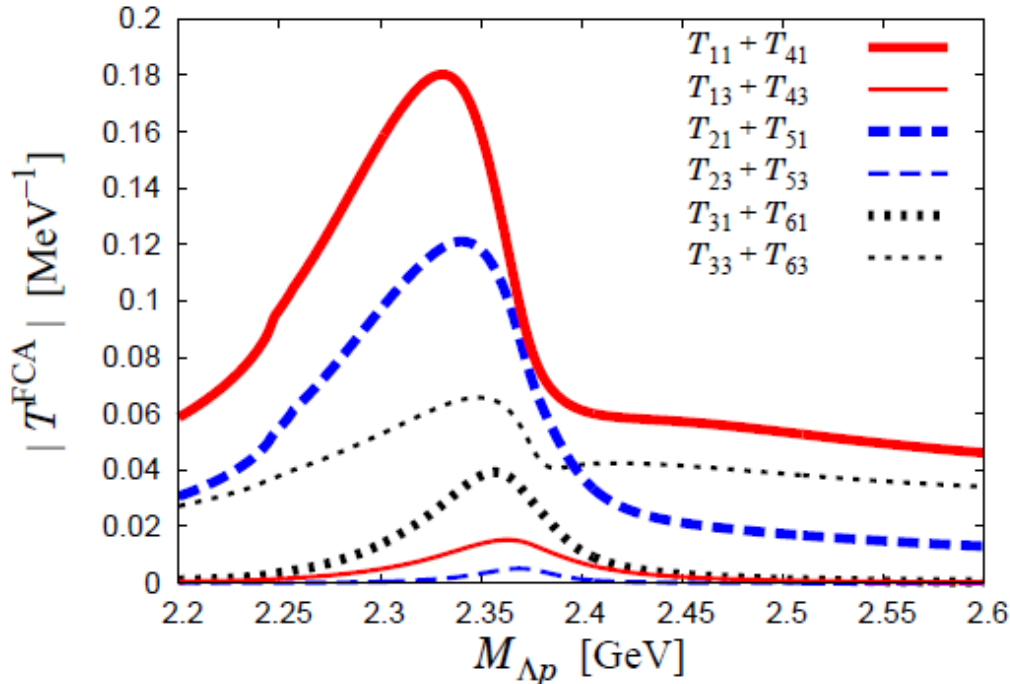
$$\mathcal{T}_1 = i \left( \chi_n^\dagger \chi \right) \left( \chi_p^\dagger \chi_\uparrow \right) T_1^{(K^- n \rightarrow K^- n)}(w_1, \cos \theta_1) \tilde{V} \int \frac{d^3 q}{(2\pi)^3} \mathcal{F}(q) q \left( \chi_\Lambda^\dagger \sigma \chi_\downarrow \right)$$

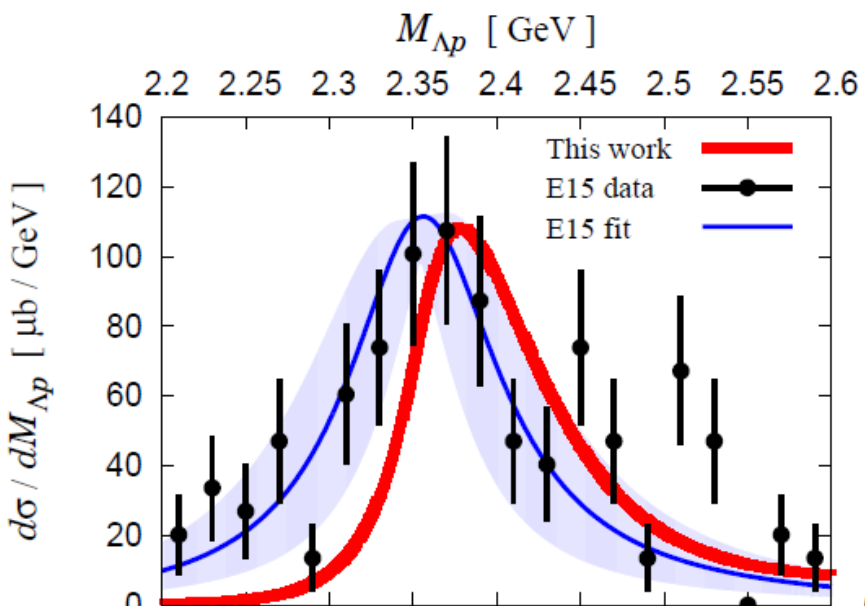
$$\times \left[ \frac{T_{11}^{\text{FCA}} + T_{41}^{\text{FCA}}}{(q^0)^2 - \omega_{K^-}(q)^2} + \frac{T_{13}^{\text{FCA}} + T_{43}^{\text{FCA}}}{(q^0)^2 - \omega_{\bar{K}^0}(q)^2} \right] \int \frac{d^3 p}{(2\pi)^3} \frac{\tilde{\Psi}(p_\lambda, p_\rho)}{(p^0)^2 - \omega_{K^-}(p)^2 + im_{K^-} \Gamma_K},$$

.....

$$\mathcal{T}_6 = -i \left( \chi_n^\dagger \chi_\downarrow \right) \left( \chi_p^\dagger \chi_\uparrow \right) T_1^{(K^- p \rightarrow \bar{K}^0 n)}(w'_1, \cos \theta'_1) \tilde{V} \int \frac{d^3 q}{(2\pi)^3} \mathcal{F}(q) q \left( \chi_\Lambda^\dagger \sigma \chi \right)$$

$$\times \left[ \frac{T_{31}^{\text{FCA}} + T_{61}^{\text{FCA}}}{(q^0)^2 - \omega_{K^-}(q)^2} + \frac{T_{33}^{\text{FCA}} + T_{63}^{\text{FCA}}}{(q^0)^2 - \omega_{\bar{K}^0}(q)^2} \right] \int \frac{d^3 p}{(2\pi)^3} \frac{\tilde{\Psi}(p_\lambda, p_\rho)}{(p^0)^2 - \omega_{\bar{K}^0}(p)^2 + im_{\bar{K}^0} \Gamma_K}$$

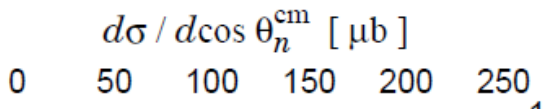
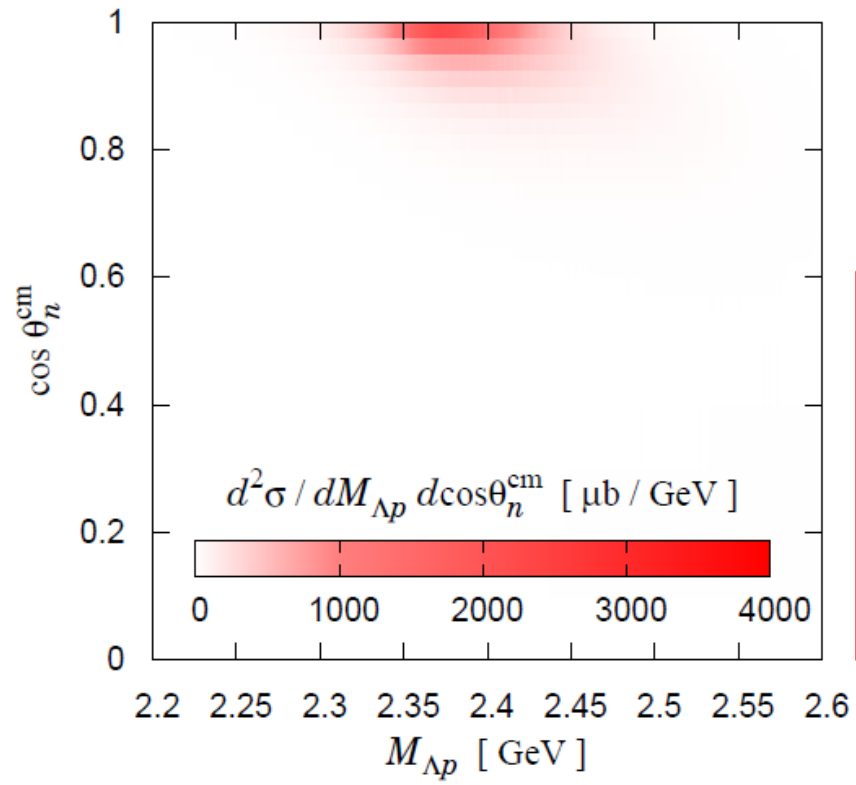


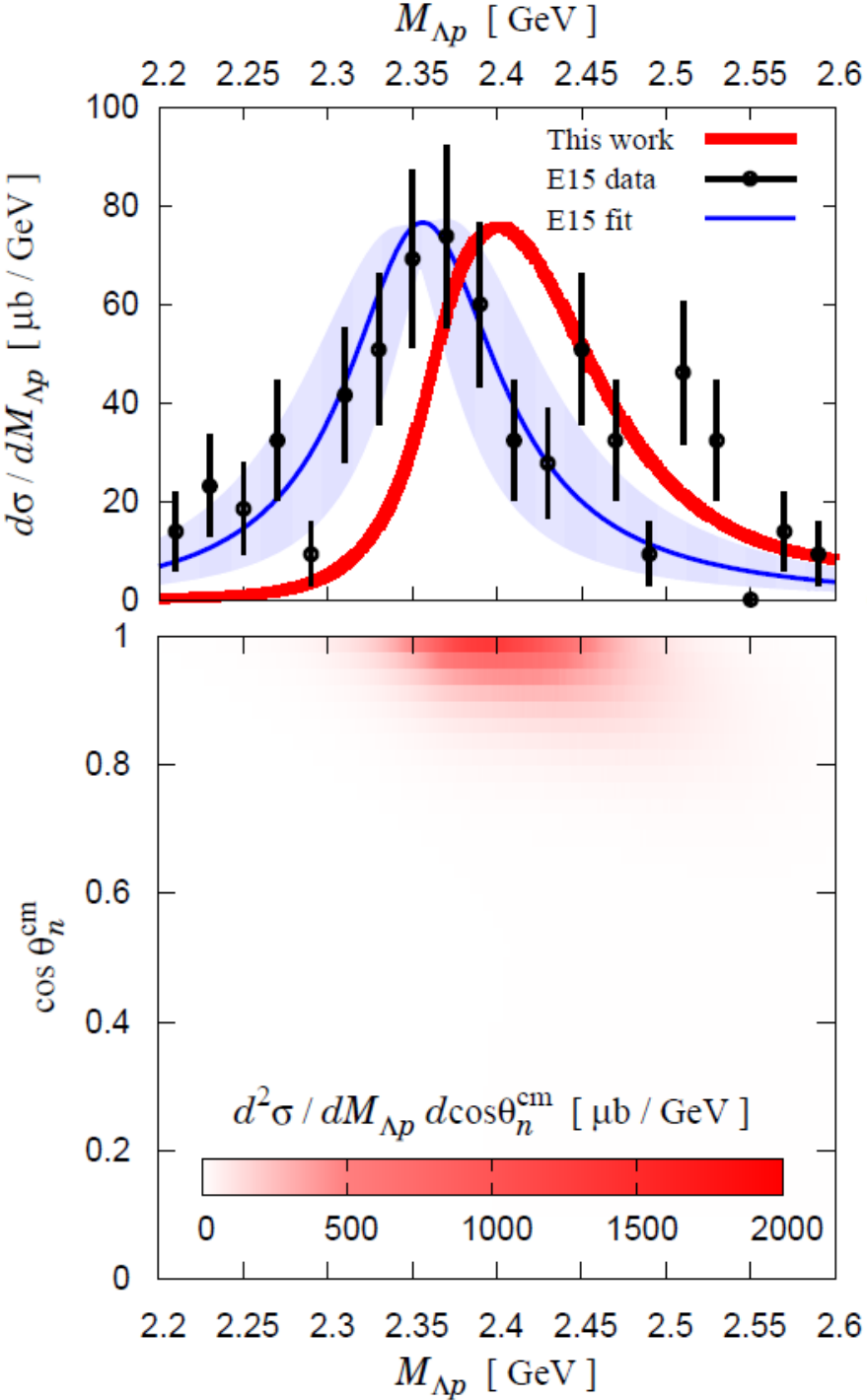


Option A

Watson approach

$$q^0 = p_{\Lambda}^{\prime 0} - \left( m_p - \frac{B_{^3\text{He}}}{3} \right)$$

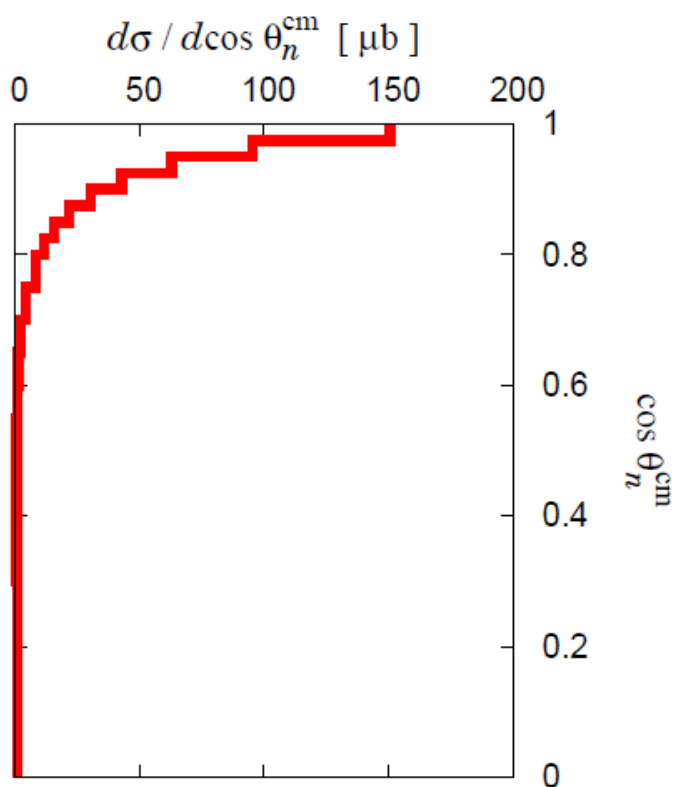




Option B

Truncated Faddeev approach

$$p^0 = q^0 + p_p'^0 - \left( m_p - \frac{B_{3\text{He}}}{3} \right)$$



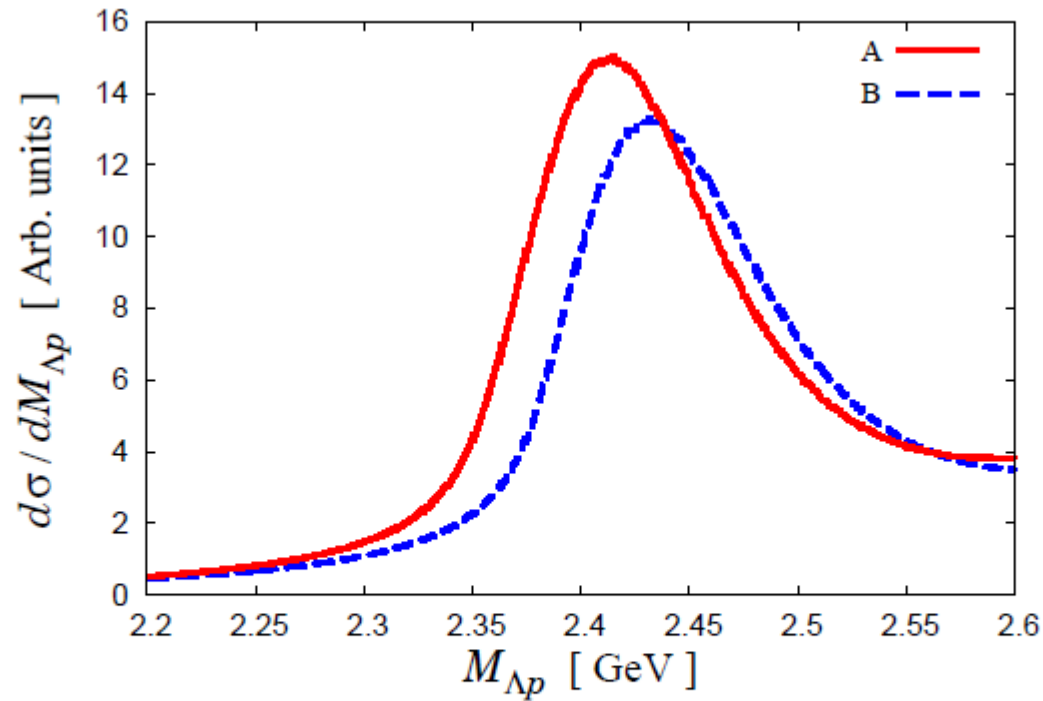
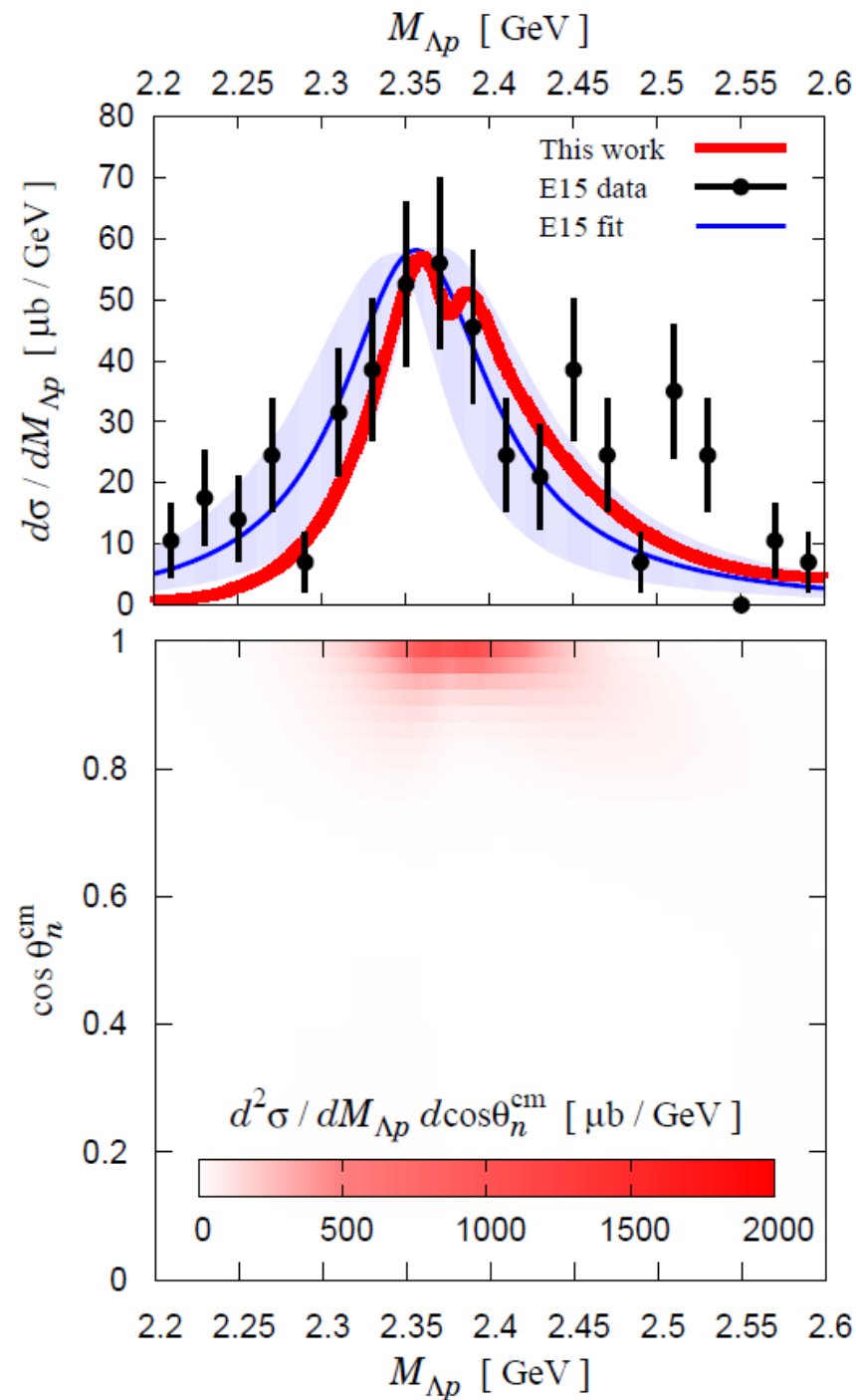


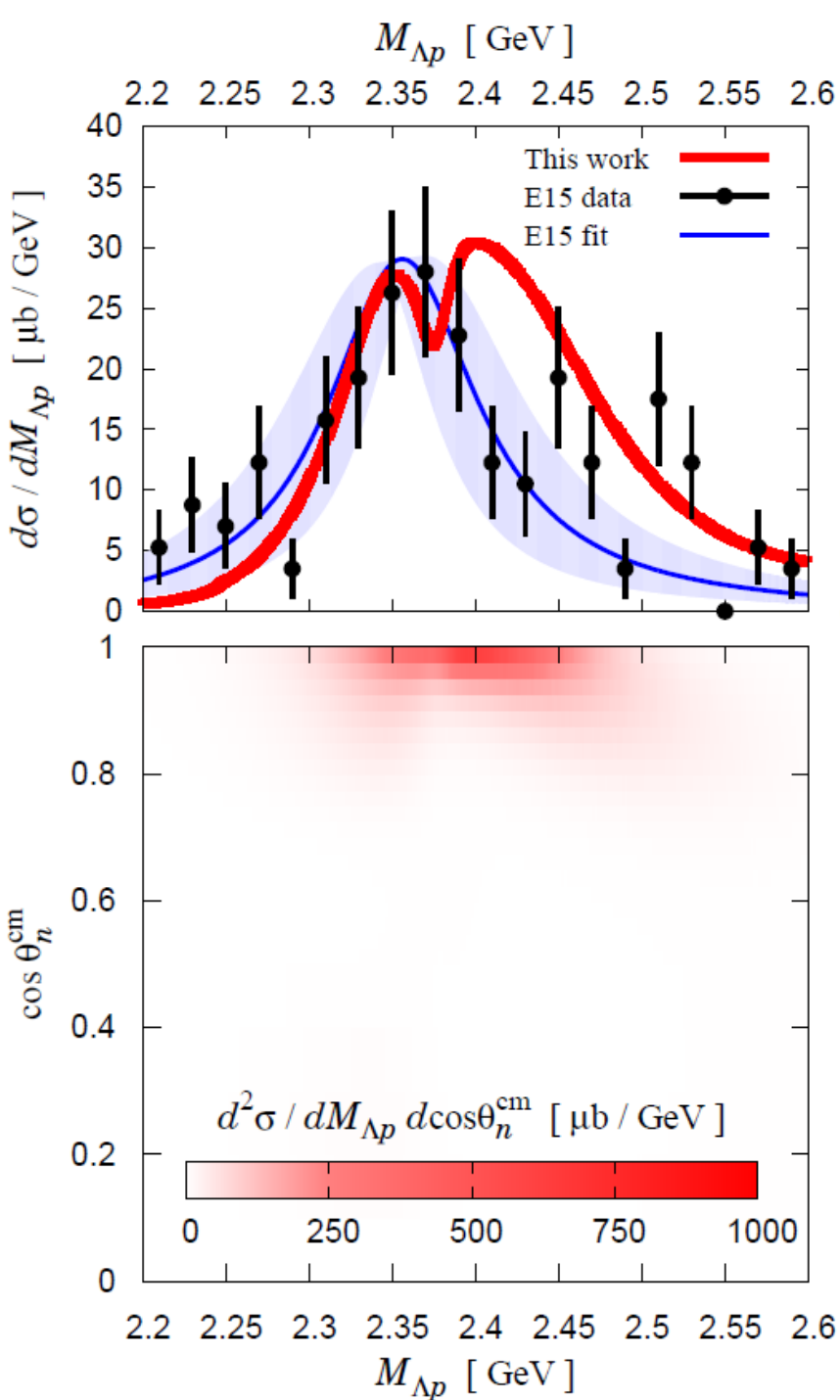
**Fig. 7** Mass spectrum for the  $\Lambda p$  invariant mass of the in-flight  ${}^3\text{He}(K^-, \Lambda p)n$  reaction with a constant  $T_2$ .

This figure shows that the shape is mostly induced by setting the Kbar propagator on shell after the first rescattering. Not due to the  $\Lambda(1405)$ , which is not here.

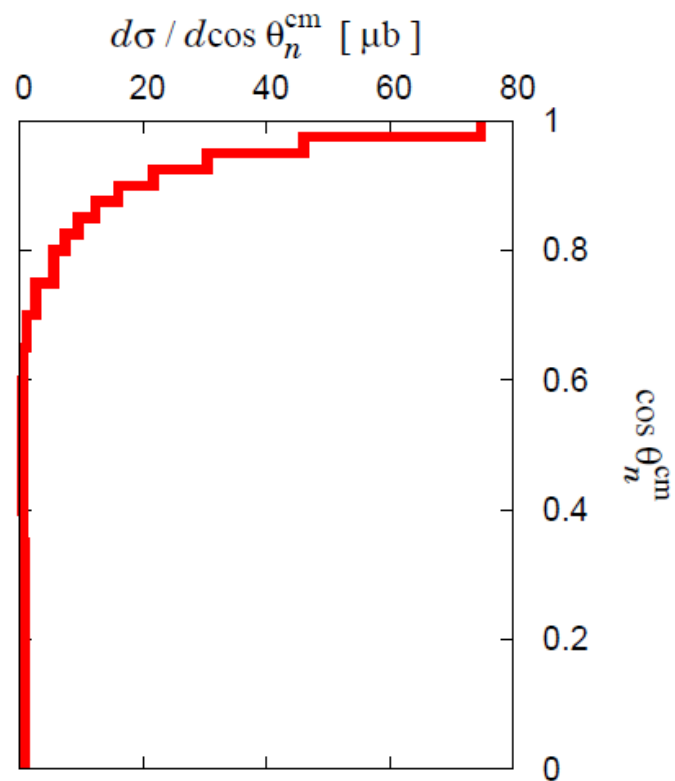


Option A

Results including  $K\bar{a}$  rescattering that leads to the binding of the  $K\bar{a}$  NN system



Option B

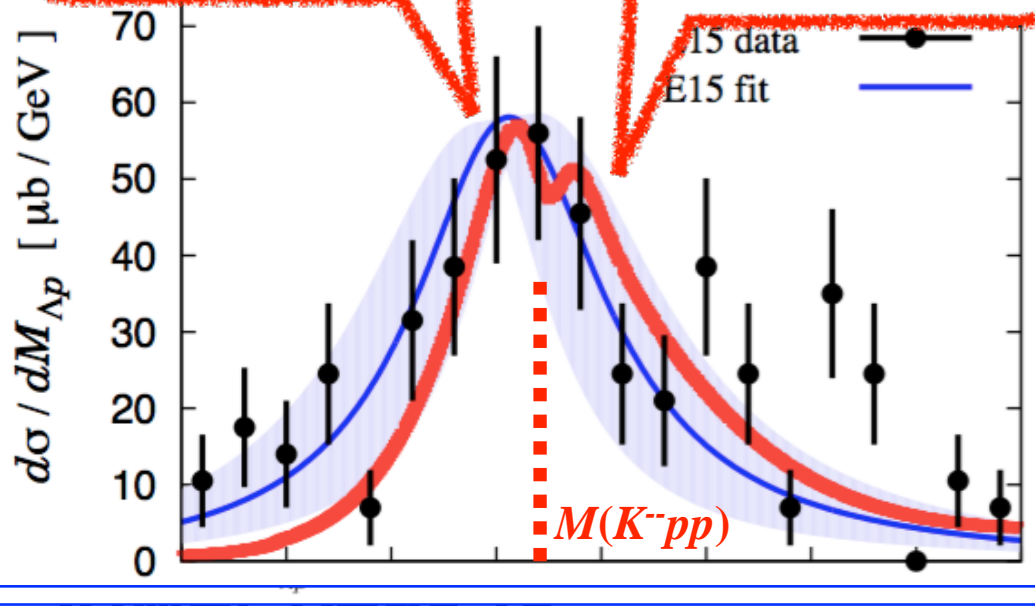
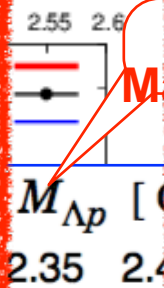
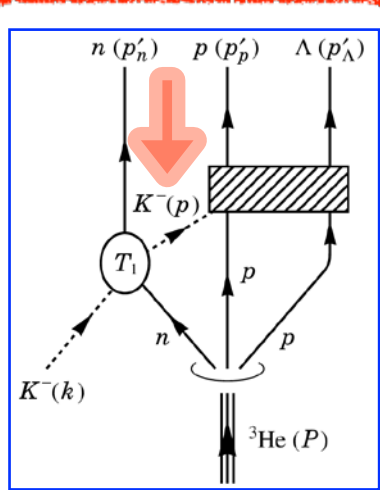
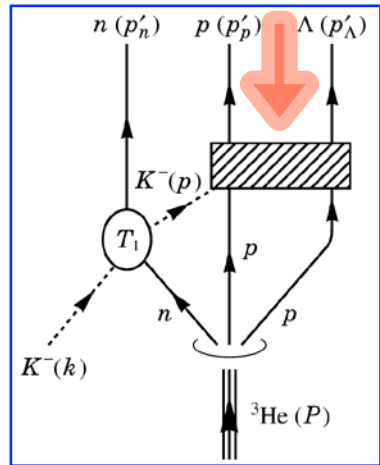


# 3. $KNN$ bound state

## Numerical results ++

### spectrum and cross

late



□ One

Our

a

--- The

lower peak is

The integrated strength is  $\sigma = 7 \mu\text{b}$ , in also good agreement with experiment

Our conclusion would be that the peak observed gives support to the existence of the so much searched  $\bar{K}$  NN state.

The agreement of our results with experiment would say that

$B \sim 20 \text{ MeV}$  and  $\Gamma \sim 80 \text{ MeV}$

Similar to Dote, Hyodo, Weise (include  $K^-$  absorption perturbatively)

Ikeda, Sato with energy dependent potential

Barnea, Gal, Liverts

But the width is bigger because of the accurate evaluation of  $K^-$  absorption